The optimization and application of photodynamic diagnosis and autofluorescence imaging in tumor diagnosis and guided surgery: current status and future prospects

Wei Wan[1†], Huiquan Liu[1†], Junrong Zou[2†], Tianpeng Xie[3], Guoxi Zhang[3], Weihai Ying[4] and Xiaofeng Zou[1,2,3]*

[1]The First Clinical College, Gannan Medical University, Ganzhou, Jiangxi, China, [2]Institute of Urology, The First Affiliated Hospital of Gannan Medical University, Ganzhou, China, [3]Department of Urology, The First Affiliated Hospital of Gannan Medical University, Ganzhou, China, [4]School of Biomedical Engineering and Med-X Research Institute, Shanghai Jiao Tong University, Shanghai, China

Photodynamic diagnosis (PDD) and autofluorescence imaging (AFI) are emerging cancer diagnostic technologies that offer significant advantages over traditional white-light endoscopy in detecting precancerous lesions and early-stage cancers; moreover, they hold promising potential in fluorescence-guided surgery (FGS) for tumors. However, their shortcomings have somewhat hindered the clinical application of PDD and AFI. Therefore, it is imperative to enhance the efficacy of PDD and AFI, thereby maximizing their potential for practical clinical use. This article reviews the principles, characteristics, current research status, and advancements of PDD and AFI, focusing on analyzing and discussing the optimization strategies of PDD and AFI in tumor diagnosis and FGS scenarios. Considering the practical and technical feasibility, optimizing PDD and AFI may result in an effective real-time diagnostic tool to guide clinicians in tumor diagnosis and surgical guidance to achieve the best results.

1 Introduction

Cancer poses a serious threat to global human health and has surpassed cardiovascular diseases as the leading cause of death in economically developed countries while remaining a major cause of mortality in developing countries (1). According to the estimates of GLOBOCAN (2), approximately 20 million new cases of cancer were recorded in 2022,

with nearly 9.7 million cancer-related deaths. Considering the growing incidence and mortality rates of cancer, improving cancer detection to achieve early diagnosis and treatment plays a crucial role in enhancing the prognosis of cancer patients. Fluorescence imaging techniques, such as photodynamic diagnosis (PDD) and autofluorescence imaging (AFI), have demonstrated significant advantages and potential in the early detection of cancer (3, 4).

Over the past few decades, significant advancements have been made in the application of fluorescence imaging technology in cancer diagnosis, particularly in the field of gastrointestinal tumor imaging, as well as in the diagnosis of tumors in the respiratory tract, skin, and bladder (5–8). Currently, fluorescence imaging plays a pivotal role in tumor diagnosis, surgical guidance, and intraoperative margin assessment, especially in the early diagnosis of cancer and intraoperative precision localization, thereby improving patient prognosis (9, 10). In traditional cancer surgery, decisions are mainly based on imaging data, the visual appearance of the tumor, and palpation. In contrast, PDD and AFI provide real-time, convenient, and accurate fluorescent image guidance for surgery (4, 6). Traditional endoscopy can only detect lesions based on the overall morphological changes, which is prone to missed diagnosis (11). However, PDD and AFI can identify precancerous changes and early tumors by examining the microstructural, biochemical, and molecular characteristics.

In addition, The ideal optical diagnostic techniques are non-invasive, objective, and reusable, offering high diagnostic accuracy and low toxicity. Nonetheless, no single optical imaging technique incorporates all these properties. Currently, optimizing or refining detection techniques has become a routine practice in the process of cancer diagnosis and surgical excision (12). Therefore, the optimization of PDD and AFI is of great clinical significance for improving the diagnosis and surgical guidance of traditional endoscopy in tumors.

2 Photodynamic diagnosis

2.1 PDD principles and characteristics

Photodynamic diagnosis (PDD), also known as fluorescence endoscopy, is an optical diagnostic technique that relies on an exogenous probe, such as a photosensitizer (PS), as a contrast mechanism to indicate pathological tissue (13). PS is injected, which is selectively accumulated in cancer cells, and exposure to excitation light of a certain wavelength triggers a unique fluorescence (14) (Figure 1). Thus, the fluorescence produced by PS differentiates between normal and abnormal tissue (14).

Notably, PDD uses a PS that has a high affinity for tumor tissue, is highly specific, and is primarily excited in the lower visible blue wavelength range. Still, the activation of PS in the excited singlet state is transient, with a lifespan typically ranging from a few nanoseconds to a few picoseconds. This process does not induce cell signal death pathways, and can only be used for fluorescence diagnosis, without causing cell damage (15). Moreover, PDD can be used to visualize biological tissues and identify disease areas. Moreover, multiple clinical trials of PDD have shown that its tumor-detection capabilities exceed that of white-light endoscopy (WLE) (16, 17), which greatly improves the early diagnosis of tumors and the prognosis.

2.2 The application and shortcomings of PDD

Currently, PDD technology is widely applied in the diagnosis of clinical tumors and fluorescence-guided surgery (FGS) (18, 19). PS plays an essential role in the PDD process. The compound selectively accumulates in tumor cells and is activated by light of a specific wavelength to trigger fluorescence, thereby promoting
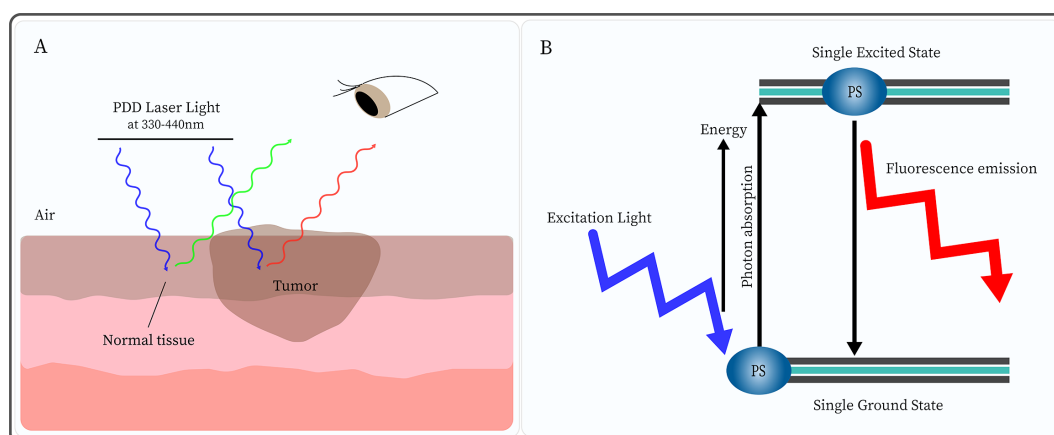
FIGURE 1
Photodynamic diagnosis (PDD) is based on the different concentrations of photosensitizer (PS) in normal and tumor tissues. **(A)** After injection of PS, under PDD laser light (330–440nm) irradiation, normal tissue emits green fluorescence while tumor tissue displays red fluorescence. **(B)** Under excitation light irradiation, the PS molecule absorbs energy from the ground state to the single excited state. Subsequently, the PS returns to the ground state while emitting light of a higher wavelength (lower energy) than that used for excitation.

effective PDD (20). In the PDD of tumors, the most commonly used PSs (mainly second-generation) include 5-aminolevulinic acid (5-ALA) (21), hexaminolevulinate (HAL) (22), methylene blue (23), and indocyanine green (ICG) (24), etc. The classification and characteristics of PS are shown in Table 1.

5-ALA is the most extensively studied photosensitizer to date and has been approved by the European Union since 2007 for use in fluorescence-guided resection of malignant gliomas (25). However, in a systematic retrospective analysis of FGS applications to 467 low-grade gliomas, the results showed that fluorescence positivity was found in 34 out of 451 (7.3%) of grade II tumors in 5-ALA-mediated PDD; whereas in 9 out of 16 (56.2%) of grade I tumors, the mean fluorescence rate of 5-ALA was 9.2% (26). Due to lower fluorescence rates and limited local bioavailability (e.g., poor lipophilicity (27)) hinders the use of 5-ALA in daily clinical practice. Therefore, a more lipophilic PS was synthesized. Compared with 5-ALA, HAL exhibits a higher efficiency in converting to protoporphyrin IX (PpIX), stronger tissue penetration, and a higher PpIX fluorescence intensity at lower concentrations (28). In a study of 699 nonmuscle invasive bladder cancer patients, Drejer et al. (29) observed tumor recurrence within 8 months after randomization under HAL-mediated PDD and WLE examinations. Results showed 117 of 351 patients in the PDD intervention group had recurrence, while 143 of 348 in the WLE control group (P=0.049), with an odds ratio of 0.67 (P=0.02, 95% CI: 0.48-0.95). Moreover, Lapini et al. (30) The diagnostic accuracy of PDD versus WLE in bladder tumors was compared and the results showed that WLE guided biopsy had a sensitivity of 76.8%, a specificity of 36.5%, a positive predictive value of 50.9%, and a negative predictive value of 64.8%, while HAL-PDD guided biopsy had a sensitivity of 99.1% (significantly higher than that of WLE, p<0.00001), specificity 30.2% (not significantly different from WLE), positive predictive value 54.9%, and negative predictive value 97.4%. The proportion of patients correctly diagnosed with PDD and WLE was 97.9% and 88.5%, respectively (p=0.0265). This further indicated that HAL-mediated PDD has a higher detection capability for precancerous lesions and early-stage tumors compared to traditional WLE. However, the HAL excitation range falls within the visible light spectrum, and the compound has poor tissue penetration. In contrast, ICG, as a second-generation photosensitizer excited at near-infrared wavelengths, is

characterized by safety, simplicity, rapidity, and avoidance of autofluorescence interference, which has facilitated its widespread application (31–33). Shiomi et al. (34) and Bargon et al. (24) found that ICG-mediated PDD had a positive role in detecting and guiding the localization of intraoperative sentinel lymph nodes in esophageal cancer and breast cancer, respectively. Nevertheless, the clinical application of ICG-mediated PDD in tumor diagnosis and FGS still confronts several challenges. For instance, ICG exhibits a low photostability, a moderate fluorescence quantum yield, and a high plasma protein binding rate (35). Simultaneously, the *in vivo* fluorescence duration of ICG is brief. This is because free ICG has a propensity to aggregate rapidly and be eliminated from the body within the physiological environment (36), and it also demonstrates a low specificity for target tumor cells (37).

Currently, researchers are attempting to overcome the shortcomings of second-generation photosensitizers by developing probes that can specifically recognize and target tumor cells (e.g., third-generation PSs), ensuring selective recognition and enhanced diagnostic efficacy (38). Nanoparticles (NPs) have been employed with great success as passive carriers (39) for the study of third-generation PSs, such as gold nanoparticles (AuNPs), silver nanoparticles, polymer nanoparticles, and silicon-based materials (40, 41). In addition, NPs can achieve passive targeting of tumors through enhanced permeability and retention (EPR) effects. The EPR passive uptake effect allows NPs-mediated PS to move freely into the tumor microvascular system through porous blood vessels and lymphatic drainage, thereby increasing PS localization in tumor cells (42). The advantages of bioactive nanoconjugates (BNCs) of NPs bound to PSs lie in their unique physicochemical properties (e.g., EPR effect) and the ability to improve the selectivity and specific targeting of second-generation PS through chemical modification (43–45). The BNC-mediated PDD process is displayed in Figure 2.

In addition, the target cell specificity of BNCs can be significantly improved by modifying the surface of BNC to bind active targeting fractions, such as antibodies (46). For example, Deken's group (47) investigated the *in vitro* and *in vivo* antitumor efficacy of photodynamic diagnosis and therapy using BNCs targeting HER2, which were found to bind specifically to the target and showed a higher affinity for HER2-positive tumor cells. Although BNC-mediated PDD has many advantages and potential

TABLE 1 Characteristics of different generations of PSs.

PS generation	Biological characteristics	PS Example	PDD (exc)/(em)
1st PS* (Low chemical purity and stability)	Only passive uptake Low of light absorption and intracellular localization	Hematoporphyrin	(330-410 nm) / (630 nm)
2nd PS (Overall performance is better than 1st PS)	Shorter half-life Improved passive uptake and tissue light penetration Minimized adverse reactions Poor water solubility and sub-cellular localization	5-ALA HAL ICG MB	(375-490 nm) / (600-740 nm) (360-465 nm) / (610-650 nm) (780 nm) / (820-850 nm) (670 nm) / (700 nm)
3rd PS (2nd PS + Nanoparticles + Target biomolecules)	Deeper tissue light penetration Improved PS tumor cell specific uptake and localization	ZnPcS4 + AuNP + Anti-GCC mAb	(330-350 nm) / (620-640 nm)

*PS, Photosensitizer; 5-ALA, 5-Aminolevulinic acid; HAL, Hexaminolevulinate; ICG, Indocyanine green; MB, Methylene blue; ZnPcS4, Zinc sulfothiolphthalocyanine; AuNP, Gold nanoparticle.
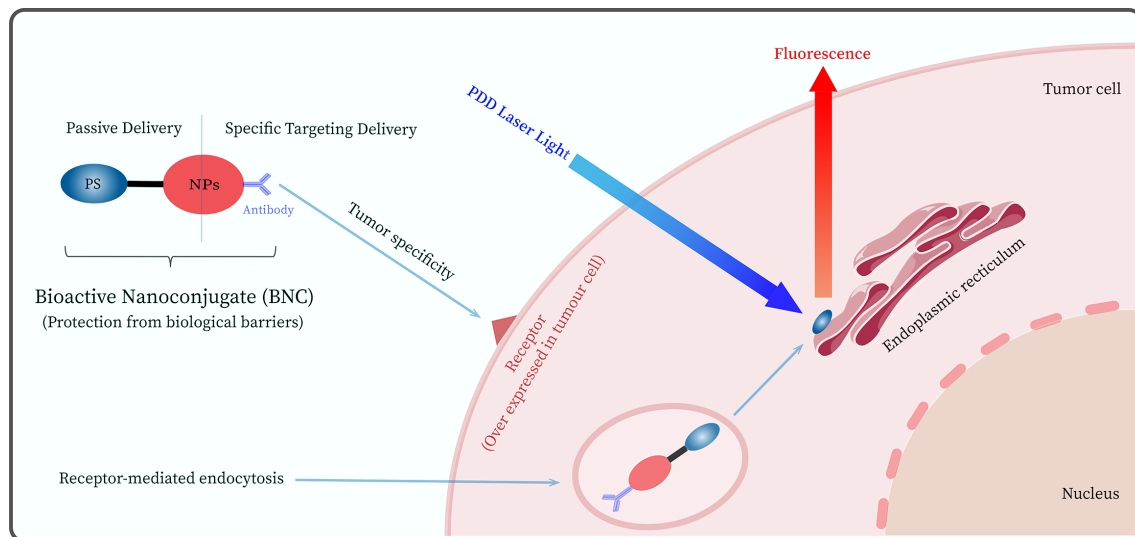
FIGURE 2
Schematic diagram of the photodynamic diagnosis PDD mediated by a bioactive nanoconjugate (BNC) composed of nanoparticles (NPs), antibody, and photosensitizer.

for clinical applications. However, it faces challenges in mediating fluorescent diagnostics and surgical navigation, such as *in vivo* environmental interference, non-specific binding, altered photophysical and chemical properties, PS drug release, and internalization issues (48–50). Moreover, PSs may have negative effects, such as pain, vomiting, and hypotension (51, 52), which limits their clinical application to a certain extent. Therefore, there is a need to further optimize BNC-mediated PDD (Such as reducing PS side effects and improving BNC optical stability, etc.) to improve its shortcomings in diagnostic and FGS application scenarios.

3 Autofluorescence imaging

3.1 AFI principles and characteristics

Autofluorescence (AF) is a widespread phenomenon in plants and animals. Cells and matrices in biological tissues contain many molecules, such as NADH, FAD, elastin, and porphyrin (53–56), which can produce AF signals corresponding to their absorption spectra when irradiated with excitation light of certain wavelengths (Figure 3).
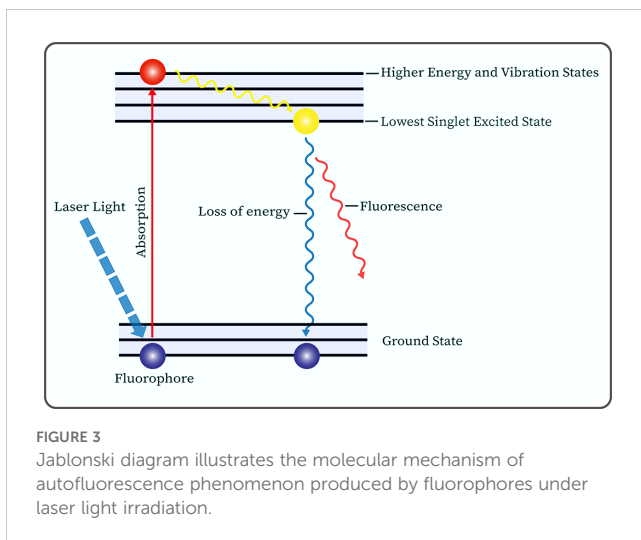
At the beginning of the last century, scientists discovered that excised tumor tissues can emit fluorescence under ultraviolet light irradiation. Subsequently, biologists have conducted extensive research on various fluorophores within organisms, revealing that the fluorescence characteristics of these molecules are related to their physicochemical properties (57, 58). Autofluorescence imaging (AFI), based on the principle of AF, involves the emission of longer wavelength AF signals by endogenous fluorophores in biological tissues under the irradiation of excitation light at specific wavelengths. These signals are then collected and processed by special sensors, which display unique fluorescent images or spectra (59). It is noteworthy that for different types of cancer, the AF intensity of cancerous tissues can be either higher or lower than that of normal tissues, e.g., melanoma's AF is higher than that in normal tissues (60), while our team's previous study found that the green AF intensity of the cancerous tissues in the lung parenchyma of lung cancer patients was significantly lower than that of the normal tissues of the lung cancer patients (61). Our study suggested that the significantly decreased green AF intensity, which may result from changes of the AF of keratins, can become a potential biomarker for non-invasive diagnosis of lung cancer (61). Therefore, normal tissues can be distinguished from cancerous tissues based on the differences in the AF images or spectral signals of the tissues to achieve the purpose of clinical diagnosis.

3.2 The application and shortcomings of AFI

AFI does not rely on exogenous probes (e.g., ICG (62)) for labeling and does not require the removal of tissue specimens for testing (63). Therefore, this method avoids liver and kidney function damage and many adverse reactions caused by exogenous tracers. In addition, the superior sensitivity of AFI compared to WLE may be related to its ability to detect subtle fluorescence changes produced by precancerous lesions or early tumors. Differences in overall fluorescence emission between normal and abnormal tissues are due to differences in fluorescent molecule concentration, metabolic state, and spatial distribution (64). And this difference in color or intensity of fluorescence emission can be captured in real-time in the AF assay for early microscopic lesions not detected by WLE.

AFI endoscopy (AFIE), which combines AFI technology with a number of endoscopes commonly used in clinical practice, has greatly improved the diagnosis of precancerous lesions and early tumors (11). Early AFIEs were mainly fiber-optic endoscopes,

FIGURE 3
Jablonski diagram illustrates the molecular mechanism of autofluorescence phenomenon produced by fluorophores under laser light irradiation.

which diagnosed pre-cancerous lesions and early tumors by detecting real-time pseudo-color images generated by AF of their own tissues. For example, Niepsuj et al. further tested the detection capability of AFIE in a study of 34 patients with short-segment Barrett's esophagus. Under AFIE and WLE examination, 109 and 136 biopsy specimens were removed from Barrett's mucosa, respectively, and it was found that the frequency of detection in AFIE-guided biopsy specimens was significantly higher than in WLE-guided biopsy specimens (8.3% vs. 0.7%; p=0.016) (65). Moreover, Sun et al. (66) conducted a meta-analysis of AF and white light bronchoscopy (WLB) for detecting bronchial carcinoma. Ten articles involving 1,830 patients' data were included. The results showed that the sensitivity of AFI was 0.92 (95% CI: 0.88-0.95), which was higher than that of WLB 0.70 (95% CI: 0.58-0.80, p<0.01). The specificity of AFI was 0.67 (95% CI: 0.51-0.80), while that of WLB was 0.78 (95% CI: 0.68-0.86, p=0.056). The positive predictive values of AFI vs. WLB were 85.0% and 76.7% respectively (p<0.05), and the negative predictive values of AFI vs. WLB were 67.6% and 70.5% respectively (p=0.06). The area under the curve (AUC) of AFI was 0.92, and that of WLB was 0.81. The Egger test yielded a P value of 0.225, indicating no publication bias. These studies demonstrated that AFI detects lesions better than WLB and has a higher sensitivity. In addition, Moriichi's team demonstrated the potential of the AFI system for the detection of precancerous lesions and early tumors in a study evaluating the grading of heterogeneous hyperplasia in colon tumors (67). Subsequently, Takeuchi et al. (68) further tested the detection ability of AFIE through a multicenter randomized controlled trial. Patients were randomly divided into the WLE group (404 patients) and the AFIE group (398 patients). The results showed that the number of flat tumors detected in the AFIE group was significantly higher than that in the WLE group (0.87 (95% CI, 0.78-0.97) vs. 0.53 (95% CI, 0.46-0.61)). In another visualization study using AFI video-endoscopy versus WLE to assess squamous cell carcinoma of the esophagus and pharynx, Suzuki et al. found that the proportion of lesions that were clearly visible on AFI video-endoscopy was significantly higher than on WLE (79% vs. 51%; p<0.05) (69). These studies demonstrated the potential of AFI for the clinical

diagnosis of precancerous lesions and early tumors. Furthermore, AFI has shown great potential in the application of FGS (70). For instance, Thomas et al. (71) achieved enhanced intraoperative adrenal visualization and effective tumor resection during adrenalectomy by introducing near-infrared AFI detection technology during surgery. In another study on intraoperative AF detection of parathyroid glands that lasted 5 years, Ladurner et al. (72) used AFI as a detection method during surgery and examined a total of 205 parathyroid glands in 117 patients. Among these, 179 glands (87.3%) were correctly identified by AF.

Nonetheless, the clinical application of AFI is circumscribed. In the current era of high-definition video endoscopes, the image quality associated with AFIE based on fiber-optic technology is considerably subpar (the fiber-optic technology provides relatively low resolution and contrast (73)), and the cumbersome imaging platform system gives rise to its unsatisfactory operability (68, 73). Meanwhile, the specificity of AFI diagnosis is relatively low, with a relatively high false positive rate; the equipment cost of AFI is higher than that of conventional WLE, and the image quality is easily disturbed by several factors (such as the internal and external environments of tissue cells, the imaging environment, the performance of signal sensors and operation techniques, etc.) (74–77). To some extent, these drawbacks limit the clinical application and adoption of AFI systems. Thus, AFI should be further optimized to improve its deficiencies in diagnostic and FGS application scenarios, which is of positive significance for improving the prognosis of cancer patients.

4 Optimization strategy for PDD and AFI

4.1 Optimization in diagnosis

Effective PDD relies on exogenous probes, selecting PS with known photophysical and pharmacokinetic properties. Additionally, exogenous PS exhibits stronger fluorescence than endogenous fluorophores. However, second-generation PSs have lower specificity (78), have significant side effects (79), and increase the cost of medication, thereby limiting the use of PDD in tumor diagnosis. In addition, PS needs to be injected before the start of PDD, and the long interval between PS administration and irradiation greatly extends the duration of diagnosis and treatment, while reducing the comfort of the therapy (80). Moreover, the dosage and method of administration for PS have not been standardized, potentially leading to excessive or insufficient dosages of PS (81). Therefore, PDD should be further optimized. For example, BNC (third-generation PSs) can reduce the adverse effects of PDD, thereby enhancing its potential for clinical application (82). Simelane's group (83) successfully prepared a BNC based on polyethylene glycolated AuNP and showed selectively improved subcellular accumulation within the target colorectal cancer, somewhat optimizing the drawbacks of insufficient PDD specificity.

Furthermore, regardless of how PS interacts with the target tissue, the continuous emission of its fluorescent signal will ultimately generate a certain level of background signal interference (84). In contrast, activatable fluorescent probes are optically silent and emit strong fluorescence only in tumors (e.g., AVB-620 (85)). Therefore, employing an activatable PS reduces the interference of background signals and improves the diagnostic ability of PDD. Nonetheless, PDD-based FGS is still limited to clinical trials due to the shortcomings of PS drugs. However, these can be circumvented by AFI, which does not rely on exogenous probes for tumor detection. Thus, the rapid metabolic clearance of PS *in vivo* as well as its adverse outcomes for patients can be significantly improved by combining PDD with AFI.

The diagnostic fundamentals of AFI and PDD are similar. The main difference is that the former does not rely on exogenous PS (Table 2), which greatly avoids unnecessary waiting times and the toxic side effects of PS. Szygula's group (86) compared the sensitivity and specificity of AFI versus PDD in the diagnosis of bladder tumors, revealing that the sensitivity and specificity of PDD were 90.91% and 66.60%, as opposed to 97.83% and 70.07% for AFI, respectively. These results demonstrate that AFI offers a more sensitive diagnosis of intravesical lesions than PDD (AFI vs. PDD; p=0.0056). However, the findings of Kriegmair et al. (70) and Kuiper et al. (87) revealed that AFI had low specificity in the diagnosis of flat tumors. This may be attributed to the differences in AFI images or spectra being affected by the internal and external environment of tissue cells (such as the concentration of fluorophores, mucosal thickness, blood concentration, etc.) and their absorption and scattering of light (76, 88). Therefore, AFI requires further optimization to minimize the impact of hemoglobin absorption spectra (89).

Moreover, AFI is not as effective as narrowband imaging (NBI) (90) in observing submucosal blood vessels and mucosal morphology, thus combining with NBI may further improve the ability of AFI in tumor diagnosis (91). Additionally, fluorescence intensity is an important parameter in tumor diagnosis with AFI or PDD. However, the fluorescence emission spectra of the fluorophores or PS of interest often overlap with those of other fluorophores in the body, which poses a certain difficulty in distinguishing between them. In contrast, fluorescence lifetime measurements utilize not only the fluorescence intensity of the fluorophore but also its fluorescence lifetime (92). Compared to fluorescence intensity measurements, fluorescence lifetime measurements provide additional information about the sample and facilitate the differentiation between scattered light and potentially endogenous fluorophores (93), and often avoid some of the factors that affect fluorescence intensity measurements (such as photobleaching, concentration, wavelength, etc.) (94). Therefore, combining fluorescence lifetime measurement technology can further optimize the fluorescence diagnostic capabilities of PDD and AFI. In the past several years, artificial intelligence (AI) technology has made profound impact on clinical medicine (95), including fluorescence-based diagnostics (96). Currently, AI technologies are widely used to enhance fluorescence imaging, process large amounts of complex and abstract data, perform pattern recognition and image analysis, and provide intelligent diagnosis (95, 97). This somewhat ameliorates the poor imaging quality due to the inadequacy of fluorescent probes. Therefore, a combined strategy with AI may overcome technical barriers and improve the diagnostic accuracy of AFI with PDD to meet the requirements of precision cancer surgery.
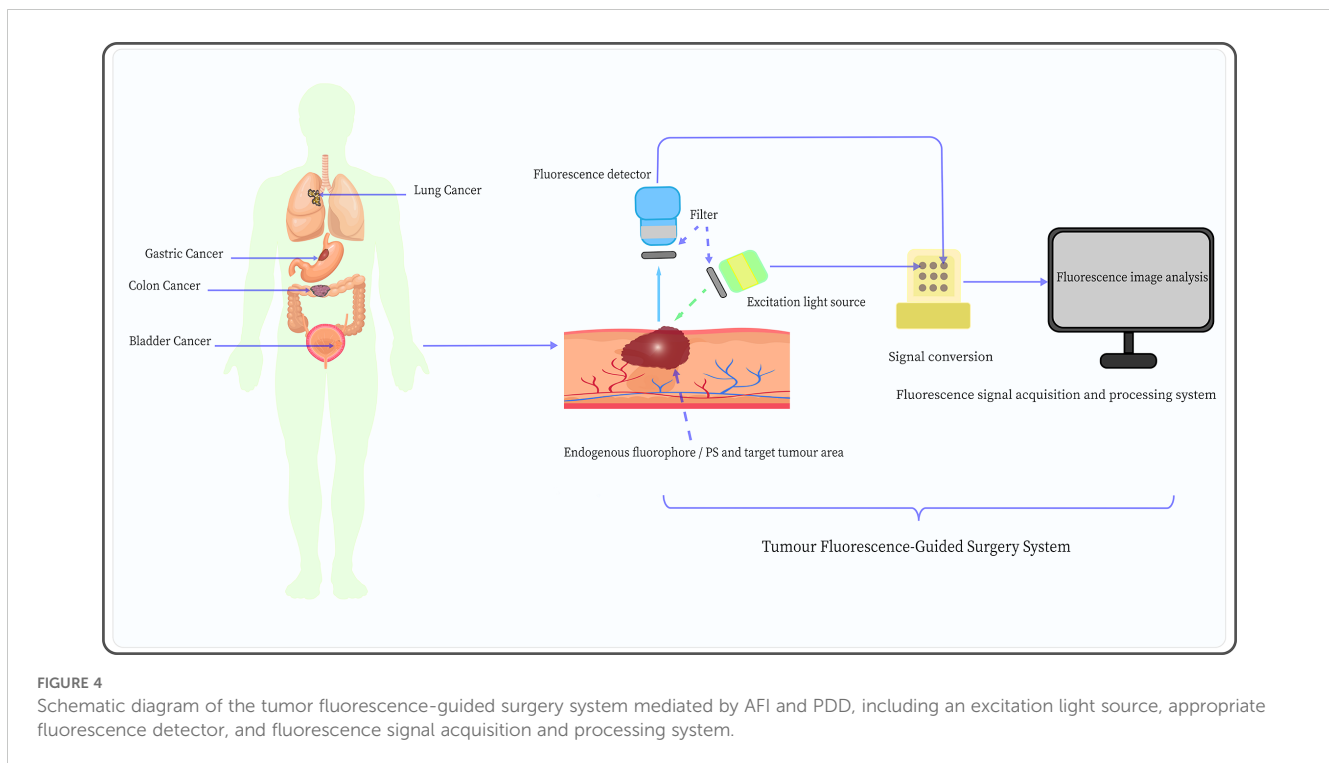
4.2 Optimization in FGS

The FGS system employing PDD and AFI mainly consists of three components: the excitation light source, the signal detector, and the signal acquisition and processing system, as shown in Figure 4. These fluorescence-related components are primarily based on mature technologies and methods that have been widely used in fluorescence spectroscopy and microscopy (98). However, the components of the fluorescence imaging system have some shortcomings that limit their application in FGS. Therefore, each fluorescence imaging system component should be further optimized to enhance the application of PDD and AFI in FGS.

Common excitation light sources for PDD and AFI include traditional light sources (mercury arc lamp systems) and light-emitting diodes (LEDs). Compared to traditional light sources,

TABLE 2 Characteristics of autofluorescence imaging and photodynamic diagnosis.

Technology	Principle	Fluorescent probe	Advantages and Disadvantages	Application scenario
AFI*	Tissue endogenous fluorophores can produce Autofluorescence signals corresponding to their absorption spectra when irradiated with a certain wavelength of excitation light	NADH FAD Collagen Keratin PpIX and Porphyrins	Advantages: Real-time, rapid, without PS, economical and prevent the negative effects of non–uniform distributions of the probes Disadvantages: Low fluorescence intensity, poor specificity and tissue penetration	Diagnosis / Fluorescence Guided Surgery
PDD	This optical diagnostic technique employs PS as a contrast mechanism for the identification of pathological tissue	5-ALA HAL ICG BNC	Advantages: High specificity, clear imaging and deep tissue penetration Disadvantages: Time-consuming, poisonous side effect and rapid clearance of PS	Diagnosis / Fluorescence Guided Surgery

*AFI, Autofluorescence imaging; PDD, Photodynamic diagnosis; PS, Photosensitizer; 5-ALA, 5-Aminolevulinic acid; HAL, Hexaminolevulinate; ICG, indocyanine green; NADH, Nicotinamide adenine dinucleotide; FAD, Flavin adenine dinucleotide; PpIX, Porphyrins IX; BNC, Bioactive Nanoconjugate.

FIGURE 4
Schematic diagram of the tumor fluorescence–guided surgery system mediated by AFI and PDD, including an excitation light source, appropriate fluorescence detector, and fluorescence signal acquisition and processing system.

LEDs are characterized by longer lifespan, narrower bandwidth emission (typically 20-30 nm), and higher signal-to-noise ratio (99). However, the narrower bandwidth implies that LEDs are not suitable for use with fluorophores with small Stokes shifts. The laser light sources have high selectivity in wavelength, which is typically much more intense; even if the wavelength does not perfectly match that of the target fluorophore, these light sources can still trigger fluorescence, such as laser diodes (100) and super-continuum laser sources (101). Nevertheless, the size and cost of laser light sources are higher than those of LEDs, which limits their application in FGS. Therefore, new laser light sources should be optimized to overcome their bulky size, simplify systems, and decrease cost in the application of PDD and AFI in FGS.

Fluorescence signal detectors are essential components of fluorescence imaging systems. Photomultiplier tubes (PMTs) are the most commonly used non-photon number-resolving detectors in biology and medicine and are characterized by high gain, low noise, fast response, and low-temperature sensitivity (102). Nonetheless, PMTs are bulky in size, require a high-voltage power supply, and are sensitive to magnetic fields (77). In contrast, silicon photomultipliers (SiPMs) have the advantages of small size, low energy and bias voltage requirements, high quantum efficiency, and insensitivity to magnetic fields, and they are relatively less expensive (103). To some extent, SiPMs provide an excellent alternative solution to traditional PMT detectors. Meanwhile, the development of some photon number resolving (PNR) detectors, such as supercon-ducting nanowire single-photon detectors (104) and transition edge sensors (105), has greatly improved the negative impact on experiments caused by the lack of PNR capability in non-PNR detectors (e.g., SiPM). Additionally, the development of charge-coupled device (CCD) cameras based on

semiconductor materials, including electron-multiplying CCD (106), has allowed detectors to amplify signals on the chip and bypass readout noise to maintain high sensitivity at high speeds. This effectively enables real-time imaging, particularly the visualization of the structure of target tissues through real-time fluorescence intensity signals, and has become one of the most commonly used detectors in the FGS systems (107). Furthermore, the complementary metal-oxide-semiconductor can provide higher image acquisition speeds, lower power consumption, and is less costly to manufacture than CCD (77). In conclusion, semiconductor, PNR, and non-PNR detectors each have their advantages; the development of suitable fluorescence detectors is an important strategy to optimize the application of PDD and AFI in FGS.

Currently, the fluorescence signal acquisition and processing system mainly applies the fluorescence imaging and fluorescence spectroscopy methods. The former method collects AF images of different tissues through detectors and directly visualizes tumor cells based on the fluorescence images (108). This approach is simple, intuitive, has a large detection range, can diagnose in real-time, and does not require complex equipment, which is very favorable for clinical applications. Kriegmair et al. (70) used pseudocolor image processing to display composite autofluorescent images to differentiate between normal and cancerous tissues, achieving a diagnostic sensitivity and specificity of 96.7% and 53.8%, respectively. However, the fluorescence imaging method presents many disadvantages, such as the time-consuming image analysis, which is highly subjective, and the quality of the image being easily affected by the surrounding environment.

On the other hand, the fluorescence spectroscopy method is based on the difference in fluorescence intensity determined by

collecting AF spectra from different tissues (109). Compared to the fluorescence imaging method, the fluorescence spectroscopy method is more rigorous and provides higher specificity as it does not need to be interpreted. Moreover, the spectral signals are rich in information, including various types of lesions, degree of tumor differentiation, and tissue subtypes (110). For example, Schuty et al. (111) analyzed the AF differences between melanoma, nevus, and normal skin by hyperspectral imaging and spectral vector analysis. The results indicated that spectral vector analysis has great potential for the diagnosis of melanoma. However, fluorescence spectroscopy also has some shortcomings, such as high equipment costs, complex structure, and the inability to visually display lesions. Moreover, this method is not as precise and convenient as fluorescence imaging in guiding surgical positioning. Therefore, combining fluorescence spectroscopy with fluorescence imaging may represent a potential approach to the FGS process.

Furthermore, in the field of FGS, the application of AI technology can enhance image recognition and provide surgical planning and decision making, ultimately achieving accuracy and safety in FGS (112). For example, Hardy et al. assessed the diagnostic efficacy of machine learning (ML) on regions of interest (ROI) in ICG-mediated FGS for 24 patients with colorectal liver metastases (CRLM). The results showed that the ML algorithms achieved a classification accuracy of 97.2% for CRLM ROIs (n = 132) within the 90s of ICG injection and all benign lesion ROIs (n = 6). The "Optimized Tree" classifier demonstrated an average accuracy of 97.2%, with a positive predictive value of 92.3% for benign lesions (113). Meanwhile, neural networks (NNs), as a branch of ML, mimics the structure of the human brain and extracts data features through hierarchical processing with self-learning and optimization capabilities. Compared with traditional statistical methods, NNs are superior in pattern recognition and calibration, reducing individual differences in fluorescent features (97). For example, convolutional neural networks (114) effectively process the fluorescence images generated by the FGS process through image processing, segmentation, feature extraction, and classification, and finally improves the accuracy and diagnostic efficacy of FGS. Finally, the trend of optimizing PDD and AFI by refining multiple parameters in fluorescence imaging systems will continue into the foreseeable future, as diagnostic and FGS applications are poised to reap significant benefits from the optimization strategy.

5 Conclusions

Fluorescence imaging, as an emerging technology for tumor diagnosis, facilitates timely detection and treatment of cancer. This review systematically describes the current research status and progress of PDD and AFI, highlighting the clinical application limitations of PDD and AFI for tumor diagnosis and FGS. The optimization of fluorescent probes, improvement of fluorescent imaging systems, and combined diagnostic strategies of PDD and AFI can largely improve their shortcomings in diagnosis and FGS.

However, well-designed and substantial clinical studies are still needed to further substantiate this perspective. Further optimization introduces certain technical challenges to the application of PDD and AFI, such as the need to balance the optimal excitation wavelengths for PDD and AFI while reducing the signal-to-noise ratio, avoiding interference from ambient light in imaging, and optimization of AI-based fluorescent signal processing algorithms, etc. With further preclinical research and clinical trials, we believe that optimized PDD and AFI will be widely applied in clinical practice.

Author contributions

WW: Conceptualization, Investigation, Software, Writing – original draft. HL: Writing – review & editing. JZ: Investigation, Supervision, Writing – review & editing. TX: Formal Analysis, Supervision, Writing – review & editing. GZ: Supervision, Validation, Writing – review & editing. WY: Formal Analysis, Methodology, Writing – review & editing. XZ: Conceptualization, Methodology, Supervision, Writing – review & editing, Writing – original draft.

Funding

Conflict of interest

The authors declare that the research was conducted in the absence of any commercial or financial relationships that could be construed as a potential conflict of interest.

Generative AI statement

The author(s) declare that no Generative AI was used in the creation of this manuscript.

Publisher's note

All claims expressed in this article are solely those of the authors and do not necessarily represent those of their affiliated organizations, or those of the publisher, the editors and the reviewers. Any product that may be evaluated in this article, or claim that may be made by its manufacturer, is not guaranteed or endorsed by the publisher.

References

1. Bray F, Laversanne M, Weiderpass E, Soerjomataram I. The ever-increasing importance of cancer as a leading cause of premature death worldwide. *Cancer*. (2021) 127:3029–30. doi: 10.1002/cncr.33587

2. Bray F, Laversanne M, Sung H, Ferlay J, Siegel RL, Soerjomataram I, et al. Global cancer statistics 2022: GLOBOCAN estimates of incidence and mortality worldwide for 36 cancers in 185 countries. *CA Cancer J Clin*. (2024) 74:229–63. doi: 10.3322/caac.21834

3. Bochynek K, Aebisher D, Gasiorek M, Cieslar G, Kawczyk-Krupka A. Evaluation of autofluorescence and photodynamic diagnosis in assessment of bladder lesions. *Photodiagnosis Photodyn Ther*. (2020) 30:101719. doi: 10.1016/j.pdpdt.2020.101719

4. Sehnem L Jr., Noureldine SI, Avci S, Isiktas G, Elshamy M, Saito Y, et al. A multicenter evaluation of near-infrared autofluorescence imaging of parathyroid glands in thyroid and parathyroid surgery. *Surgery*. (2023) 173:132–7. doi: 10.1016/j.surg.2022.07.057

5. Sasaki M, Tanaka M, Ichikawa H, Suzuki T, Nishie H, Ozeki K, et al. 5-aminolaevulinic acid (5-ALA) accumulates in GIST-T1 cells and photodynamic diagnosis using 5-ALA identifies gastrointestinal stromal tumors (GISTs) in xenograft tumor models. *PloS One*. (2021) 16:e0249650. doi: 10.1371/journal.pone.0249650

6. Wada H, Yamamoto T, Morimoto J, Sakairi Y, Suzuki H, Nakajima T, et al. Near-infrared-guided pulmonary segmentectomy after endobronchial indocyanine green injection. *Ann Thorac Surg*. (2020) 109:396–403. doi: 10.1016/j.athoracsur.2019.08.083

7. Kwiatek S, Kawczyk-Krupka A, Mańka E, Cieślar G, Sieroń A, Stanek A. Can fluorescence and autofluorescence imaging be useful in diagnosis of basal cell cancer? Proposition of algorithms. *Photodiagnosis Photodyn Ther*. (2020) 30:101697. doi: 10.1016/j.pdpdt.2020.101697

8. Kurabayashi A, Fukuhara H, Furihata K, Iwashita W, Furihata M, Inoue K. Photodynamic diagnosis and therapy in non-muscle-invasive bladder cancer. *Cancers (Basel)*. (2024) 16:2299. doi: 10.3390/cancers16132299

9. Sutton PA, van Dam MA, Cahill RA, Mieog S, Polom K, Vahrmeijer AL, et al. Fluorescence-guided surgery: comprehensive review. *BJS Open*. (2023) 7:zrad049. doi: 10.1093/bjsopen/zrad049

10. Sari Motlagh R, Mori K, Laukhtina E, Aydh A, Katayama S, Grossmann NC, et al. Impact of enhanced optical techniques at time of transurethral resection of bladder tumour, with or without single immediate intravesical chemotherapy, on recurrence rate of non-muscle-invasive bladder cancer: a systematic review and network meta-analysis of randomized trials. *BJU Int*. (2021) 128:280–9. doi: 10.1111/bju.15383

11. Bi Y, Min M, Cui Y, Xu Y, Li X. Research progress of autofluorescence imaging technology in the diagnosis of early gastrointestinal tumors. *Cancer Control*. (2021) 28:10732748211044337. doi: 10.1177/10732748211044337

12. Zhang Y, Li M, Gao X, Chen Y, Liu T. Nanotechnology in cancer diagnosis: progress, challenges and opportunities. *J Hematol Oncol*. (2019) 12:137. doi: 10.1186/s13045-019-0833-3

13. Namikawa T, Iwabu J, Munekage M, Uemura S, Maeda H, Kitagawa H, et al. Evolution of photodynamic medicine based on fluorescence image-guided diagnosis using indocyanine green and 5-aminolevulinic acid. *Surg Today*. (2020) 50:821–31. doi: 10.1007/s00595-019-01851-4

14. Matoba Y, Banno K, Kisu I, Kobayashi Y, Tsuji K, Nagai S, et al. Hysteroscopic photodynamic diagnosis using 5-aminolevulinic acid: A high-sensitivity diagnostic method for uterine endometrial Malignant diseases. *J Minim Invasive Gynecol*. (2020) 27:1087–94. doi: 10.1016/j.jmig.2019.08.012

15. Bacellar IO, Tsubone TM, Pavani C, Baptista MS. Photodynamic efficiency: from molecular photochemistry to cell death. *Int J Mol Sci*. (2015) 16:20523–59. doi: 10.3390/ijms160920523

16. Fukuhara H, Kurabayashi A, Furihata M, Setuda S, Takahashi K, Murakami K, et al. 5-aminolevulinic acid-mediated photodynamic diagnosis using fluorescence ureterorenoscopy for urinary upper tract urothelial carcinoma ∼Preliminary prospective single centre trial∼. *Photodiagnosis Photodyn Ther*. (2020) 29:101617. doi: 10.1016/j.pdpdt.2019.101617

17. Capece M, Spirito L, La Rocca R, Napolitano L, Buonopane R, Di Meo S, et al. Hexaminolevulinate blue light cystoscopy (Hal) assisted transurethral resection of the bladder tumour vs white light transurethral resection of the bladder tumour in non-muscle invasive bladder cancer (NMIBC): a retrospective analysis. *Arch Ital Urol Androl*. (2020) 92:17–20. doi: 10.4081/aiua.2020.1.17

18. Shofty B, Richetta C, Haim O, Kashanian A, Gurevich A, Grossman R. 5-ALA-assisted stereotactic brain tumor biopsy improve diagnostic yield. *Eur J Surg Oncol*. (2019) 45:2375–8. doi: 10.1016/j.ejso.2019.07.001

19. Galema HA, Meijer RPJ, Lauwerends LJ, Verhoef C, Burggraaf J, Vahrmeijer AL, et al. Fluorescence-guided surgery in colorectal cancer; A review on clinical results and future perspectives. *Eur J Surg Oncol*. (2022) 48:810–21. doi: 10.1016/j.ejso.2021.10.005

20. Picart T, Pallud J, Berthiller J, Dumot C, Berhouma M, Ducray F, et al. Use of 5-ALA fluorescence-guided surgery versus white-light conventional microsurgery for the resection of newly diagnosed glioblastomas (RESECT study): a French multicenter randomized phase III study. *J Neurosurg*. (2024) 140:987–1000. doi: 10.3171/2023.7.Jns231170

21. Harada Y, Murayama Y, Takamatsu T, Otsuji E, Tanaka H. 5-aminolevulinic acid-induced protoporphyrin IX fluorescence imaging for tumor detection: recent advances and challenges. *Int J Mol Sci*. (2022) 23:6478. doi: 10.3390/ijms23126478

22. Lotan Y, Chaplin I, Ahmadi H, Meng X, Roberts S, Ladi-Seyedian S, et al. Prospective evaluation of blue-light flexible cystoscopy with hexaminolevulinate in non-muscle-invasive bladder cancer. *BJU Int*. (2021) 127:108–13. doi: 10.1111/bju.15166

23. Tummers QR, Verbeek FP, Schaafsma BE, Boonstra MC, van der Vorst JR, Liefers GJ, et al. Real-time intraoperative detection of breast cancer using near-infrared fluorescence imaging and Methylene Blue. *Eur J Surg Oncol*. (2014) 40:850–8. doi: 10.1016/j.ejso.2014.02.225

24. Bargon CA, Huibers A, Young-Afat DA, Jansen BAM, Borel-Rinkes IHM, Lavalaye J, et al. Sentinel lymph node mapping in breast cancer patients through fluorescent imaging using indocyanine green: the INFLUENCE trial. *Ann Surg*. (2022) 276:913–20. doi: 10.1097/sla.0000000000005633

25. Traylor JI, Pernik MN, Sternisha AC, McBrayer SK, Abdullah KG. Molecular and metabolic mechanisms underlying selective 5-aminolevulinic acid-induced fluorescence in gliomas. *Cancers (Basel)*. (2021) 13(3):580. doi: 10.3390/cancers13030580

26. Bianconi A, Bonada M, Zeppa P, Colonna S, Tartara F, Melcarne A, et al. How reliable is fluorescence-guided surgery in low-grade gliomas? A systematic review concerning different fluorophores. *Cancers (Basel)*. (2023) 15:4130. doi: 10.3390/cancers15164130

27. Wu RWK, Chu ESM, Yow CMN. Evaluation of the effect of 5-aminolevulinic acid hexyl ester (H-ALA) PDT on EBV LMP1 protein expression in human nasopharyngeal cells. *Photodiagnosis Photodyn Ther*. (2020) 30:101801. doi: 10.1016/j.pdpdt.2020.101801

28. Chan KM, Vasilev K, Shirazi HS, McNicholas K, Li J, Gleadle J, et al. Biosensor device for the photo-specific detection of immuno-captured bladder cancer cells using hexaminolevulinate: An ex-vivo study. *Photodiagnosis Photodyn Ther*. (2019) 28:238–47. doi: 10.1016/j.pdpdt.2019.08.001

29. Drejer D, Moltke AL, Nielsen AM, Lam GW, Jensen JB. DaBlaCa-11: photodynamic diagnosis in flexible cystoscopy-A randomized study with focus on recurrence. *Urology*. (2020) 137:91–6. doi: 10.1016/j.urology.2019.12.002

30. Lapini A, Minervini A, Masala A, Schips L, Pycha A, Cindolo L, et al. A comparison of hexaminolevulinate (Hexvix(®)) fluorescence cystoscopy and white-light cystoscopy for detection of bladder cancer: results of the HeRo observational study. *Surg endoscopy*. (2012) 26:3634–41. doi: 10.1007/s00464-012-2387-0

31. Egloff-Juras C, Bezdetnaya L, Dolivet G, Lassalle HP. NIR fluorescence-guided tumor surgery: new strategies for the use of indocyanine green. *Int J Nanomedicine*. (2019) 14:7823–38. doi: 10.2147/ijn.S207486

32. Papet E, Pinson J, Tuech JJ. Indocyanine green fluorescent lymphography: Surgical procedure. *J Visc Surg*. (2022) 159:325–9. doi: 10.1016/j.jviscsurg.2021.12.001

33. Strigalev M, Tzedakis S, Nassar A, Dhote A, Gavignet C, Gaillard M, et al. Intra-operative indocyanine green fluorescence imaging in hepatobiliary surgery: a narrative review of the literature as a useful guide for the surgeon. *Updates Surg*. (2023) 75:23–9. doi: 10.1007/s13304-022-01388-1

34. Shiomi S, Yagi K, Iwata R, Yajima S, Okumura Y, Aikou S, et al. Lymphatic flow mapping using near-infrared fluorescence imaging with indocyanine green helps to predict lymph node metastasis intraoperatively in patients with esophageal or esophagogastric junction cancer not treated with neoadjuvant chemotherapy. *Surg endoscopy*. (2023) 37:8214–26. doi: 10.1007/s00464-023-10368-4

35. Luo S, Zhang E, Su Y, Cheng T, Shi C. A review of NIR dyes in cancer targeting and imaging. *Biomaterials*. (2011) 32:7127–38. doi: 10.1016/j.biomaterials.2011.06.024

36. Altınoğlu EI, Russin TJ, Kaiser JM, Barth BM, Eklund PC, Kester M, et al. Near-infrared emitting fluorophore-doped calcium phosphate nanoparticles for *in vivo* imaging of human breast cancer. *ACS nano*. (2008) 2:2075–84. doi: 10.1021/nn800448r

37. Satou S, Ishizawa T, Masuda K, Kaneko J, Aoki T, Sakamoto Y, et al. Indocyanine green fluorescent imaging for detecting extrahepatic metastasis of hepatocellular carcinoma. *J Gastroenterol*. (2013) 48:1136–43. doi: 10.1007/s00535-012-0709-6

38. Mfouo-Tynga IS, Dias LD, Inada NM, Kurachi C. Features of third generation photosensitizers used in anticancer photodynamic therapy: Review. *Photodiagnosis Photodyn Ther*. (2021) 34:102091. doi: 10.1016/j.pdpdt.2020.102091

39. Wang Q, Xia G, Li J, Yuan L, Yu S, Li D, et al. Multifunctional nanoplatform for NIR-II imaging-guided synergistic oncotherapy. *Int J Mol Sci*. (2023) 24:16949. doi: 10.3390/ijms242316949

40. Dhanalekshmi KI, Sangeetha K, Magesan P, Johnson J, Zhang X, Jayamoorthy K. Photodynamic cancer therapy: role of Ag- and Au-based hybrid nano-photosensitizers. *J Biomol Struct Dyn*. (2022) 40:4766–73. doi: 10.1080/07391102.2020.1858965

41. Truong DH, Tran PTT, Tran TH. Nanoparticles as carriers of photosensitizers to improve photodynamic therapy in cancer. *Pharm Dev Technol*. (2024) 29:221–35. doi: 10.1080/10837450.2024.2322570

42. Maeda H, Wu J, Sawa T, Matsumura Y, Hori K. Tumor vascular permeability and the EPR effect in macromolecular therapeutics: a review. *J Controlled Release.* (2000) 65:271–84. doi: 10.1016/S0168-3659(99)00248-5

43. Alsaab HO, Alghamdi MS, Alotaibi AS, Alzhrani R, Alwuthaynani F, Althobaiti YS, et al. Progress in clinical trials of photodynamic therapy for solid tumors and the role of nanomedicine. *Cancers (Basel).* (2020) 12:2793. doi: 10.3390/cancers12102793

44. Didamson OC, Abrahamse H. Targeted photodynamic diagnosis and therapy for esophageal cancer: potential role of functionalized nanomedicine. *Pharmaceutics.* (2021) 13:1943. doi: 10.3390/pharmaceutics13111943

45. Liu N, Chen X, Sun X, Sun X, Shi J. Persistent luminescence nanoparticles for cancer theranostics application. *J Nanobiotechnology.* (2021) 19:113. doi: 10.1186/s12951-021-00862-z

46. Yadav R, Das PP, Sharma S, Sengupta S, Kumar D, Sagar R. Recent advancement of nanomedicine-based targeted delivery for cervical cancer treatment. *Med Oncol.* (2023) 40:347. doi: 10.1007/s12032-023-02195-3

47. Deken MM, Kijanka MM, Beltrán Hernández I, Slooter MD, de Bruijn HS, van Diest PJ, et al. Nanobody-targeted photodynamic therapy induces significant tumor regression of trastuzumab-resistant HER2-positive breast cancer, after a single treatment session. *J Control Release.* (2020) 323:269–81. doi: 10.1016/j.jconrel.2020.04.030

48. Feng L, Jiang D. Fluorescent intraoperative navigation: trends and beyond. *Am J Nucl Med Mol imaging.* (2022) 12:138–42.

49. Ma F, Jia Q, Deng Z, Wang B, Zhang S, Jiang J, et al. Boosting luminescence efficiency of near-infrared-II aggregation-induced emission luminogens via a mash-up strategy of π-extension and deuteration for dual-model image-guided surgery. *ACS nano.* (2024) 18:9431–42. doi: 10.1021/acsnano.3c11078

50. Wang Y, Li Y, Zhang Z, Wang L, Wang D, Tang BZ. Triple-jump photodynamic theranostics: mnO(2) combined upconversion nanoplatforms involving a type-I photosensitizer with aggregation-induced emission characteristics for potent cancer treatment. *Advanced materials (Deerfield Beach Fla).* (2021) 33:e2103748. doi: 10.1002/adma.202103748

51. Taoka R, Yamada K, Sawanobori Y, Honda T, Osaki Y, Abe Y, et al. Oral 5-aminolevulinic acid administration before transurethral resection of bladder tumor induces perioperative nausea and vomiting. *Photodiagnosis Photodyn Ther.* (2023) 43:103707. doi: 10.1016/j.pdpdt.2023.103707

52. Okabe Y, Fukuhara Y, Matsuoka W, Nobuyuki N, Hiroshi M, Takeshi M, et al. Identification of risk factors associated with oral 5-aminolevulinic acid induced adverse events in photodynamic diagnosis-transurethral resection of bladder tumor. *Photodiagnosis Photodyn Ther.* (2024) 49:104291. doi: 10.1016/j.pdpdt.2024.104291

53. Yuan Y, Yan Z, Miao J, Cai R, Zhang M, Wang Y, et al. Autofluorescence of NADH is a new biomarker for sorting and characterizing cancer stem cells in human glioma. *Stem Cell Res Ther.* (2019) 10:330. doi: 10.1186/s13287-019-1467-7

54. Bryanskaya EO, Vinokurov AY, Dolgikh AI, Dunaev AV, Angelova PR, Abramov AY. High levels of FAD autofluorescence indicate pathology preceding cell death. *Biochim Biophys Acta Gen Subj.* (2024) 1868:130520. doi: 10.1016/j.bbagen.2023.130520

55. Li H, Yan M, Yu J, Xu Q, Xia X, Liao J, et al. *In vivo* identification of arteries and veins using two-photon excitation elastin autofluorescence. *J Anat.* (2020) 236:171–9. doi: 10.1111/joa.13080

56. Lennon ÁM, Brune L, Techert S, Buchalla W. Fluorescence spectroscopy shows porphyrins produced by cultured oral bacteria differ depending on composition of growth media. *Caries Res.* (2023) 57:74–86. doi: 10.1159/000528731

57. Georgakoudi I, Quinn KP. Optical imaging using endogenous contrast to assess metabolic state. *Annu Rev BioMed Eng.* (2012) 14:351–67. doi: 10.1146/annurev-bioeng-071811-150108

58. Georgakoudi I, Quinn KP. Label-free optical metabolic imaging in cells and tissues. *Annu Rev BioMed Eng.* (2023) 25:413–43. doi: 10.1146/annurev-bioeng-071516-044730

59. Orkin R, Sharma A, John JV, Armstrong DG. Current and future directions in fluorescence imaging-guided debridement. *Adv Wound Care (New Rochelle).* (2024). doi: 10.1089/wound.2024.0067

60. Knab A, Anwer AG, Pedersen B, Handley S, Marupally AG, Habibalahi A, et al. Towards label-free non-invasive autofluorescence multispectral imaging for melanoma diagnosis. *J biophotonics.* (2024) 17:e202300402. doi: 10.1002/jbio.202300402

61. Zhang M, Zhang J, Teng H, Zhang Q, Xiang Z, Chang Q, et al. Decreased green autofluorescence of lung parenchyma is a biomarker for lung cancer tissues. *J biophotonics.* (2022) 15:e202200072. doi: 10.1002/jbio.202200072

62. Esposito C, Coppola V, Del Conte F, Cerulo M, Esposito G, Farina A, et al. Near-Infrared fluorescence imaging using indocyanine green (ICG): Emerging applications in pediatric urology. *J Pediatr Urol.* (2020) 16:700–7. doi: 10.1016/j.jpurol.2020.07.008

63. Croce AC, Ferrigno A, Bottiroli G, Vairetti M. Autofluorescence-based optical biopsy: An effective diagnostic tool in hepatology. *Liver Int.* (2018) 38:1160–74. doi: 10.1111/liv.13753

64. Levitt JM, McLaughlin-Drubin ME, Münger K, Georgakoudi I. Automated biochemical, morphological, and organizational assessment of precancerous changes from endogenous two-photon fluorescence images. *PloS One.* (2011) 6:e24765. doi: 10.1371/journal.pone.0024765

65. Niepsuj K, Niepsuj G, Cebula W, Zieleźnik W, Adamek M, Sielańczyk A, et al. Autofluorescence endoscopy for detection of high-grade dysplasia in short-segment Barrett's esophagus. *Gastrointest Endosc.* (2003) 58:715–9. doi: 10.1016/s0016-5107(03)02018-2

66. Sun S, Yang Y, Chen M, Wang L, Pan H, Zhang X, et al. Comparison of autofluorescence and white-light bronchoscopies performed with the Evis Lucera Spectrum for the detection of bronchial cancers: a meta-analysis. *Transl Lung Cancer Res.* (2020) 9:23–32. doi: 10.21037/tlcr.2020.01.04

67. Moriichi K, Fujiya M, Sato R, Nata T, Nomura Y, Ueno N, et al. Autofluorescence imaging and the quantitative intensity of fluorescence for evaluating the dysplastic grade of colonic neoplasms. *Int J Colorectal Dis.* (2012) 27:325–30. doi: 10.1007/s00384-011-1311-8

68. Takeuchi Y, Sawaya M, Oka S, Tamai N, Kawamura T, Uraoka T, et al. Efficacy of autofluorescence imaging for flat neoplasm detection: a multicenter randomized controlled trial (A-FLAT trial). *Gastrointest Endosc.* (2019) 89:460–9. doi: 10.1016/j.gie.2018.11.012

69. Suzuki H, Saito Y, Ikehara H, Oda I. Evaluation of visualization of squamous cell carcinoma of esophagus and pharynx using an autofluorescence imaging videoendoscope system. *J Gastroenterol Hepatol.* (2009) 24:1834–9. doi: 10.1111/j.1440-1746.2009.05941.x

70. Kriegmair MC, Honeck P, Theuring M, Bolenz C, Ritter M. Wide-field autofluorescence-guided TUR-B for the detection of bladder cancer: a pilot study. *World J Urology.* (2018) 36:745–51. doi: 10.1007/s00345-017-2147-9

71. Thomas G, Kiernan CM, Willmon PA, Haugen E, Luckenbaugh AN, Barocas DA, et al. Label-free enhancement of adrenal gland visualization using near-infrared autofluorescence for surgical guidance. *World J Surg.* (2023) 47:350–60. doi: 10.1007/s00268-022-06755-y

72. Ladurner R, Lerchenberger M, Al Arabi N, Gallwas JKS, Stepp H, Hallfeldt KKJ. Parathyroid autofluorescence-how does it affect parathyroid and thyroid surgery? A 5 year experience. *Molecules.* (2019) 24:2560. doi: 10.3390/molecules24142560

73. Borovicka J, Fischer J, Neuweiler J, Netzer P, Gschossmann J, Ehmann T, et al. Autofluorescence endoscopy in surveillance of Barrett's esophagus: a multicenter randomized trial on diagnostic efficacy. *Endoscopy.* (2006) 38:867–72. doi: 10.1055/s-2006-944726

74. Falk GW. Autofluorescence endoscopy. *Gastrointest Endosc Clin N Am.* (2009) 19:209–20. doi: 10.1016/j.giec.2009.02.004

75. Odagaki T, Sakamoto T, Sekiguchi M, Sato C, Tamai N, Otake Y, et al. What is the accuracy of autofluorescence imaging in identifying non-polypoid colorectal neoplastic lesions when reviewed by trainees? A pilot study. *Dig Endosc.* (2013) 25:428–33. doi: 10.1111/j.1443-1661.2012.01400.x

76. Su L, Fonseca MB, Arya S, Kudo H, Goldin R, Hanna GB, et al. Laser-induced tissue fluorescence in radiofrequency tissue-fusion characterization. *J BioMed Opt.* (2014) 19:15007. doi: 10.1117/1.JBO.19.1.015007

77. Calabretta MM, Lopreside A, Montali L, Zangheri M, Evangelisti L, D'Elia M, et al. Portable light detectors for bioluminescence biosensing applications: A comprehensive review from the analytical chemist's perspective. *Anal Chim Acta.* (2022) 1200:339583. doi: 10.1016/j.aca.2022.339583

78. Xu J, Zhao J, Dong Y, Zhao X, Chen R, Shi Y, et al. Photodetection and safety of 5-aminolevulinic acid-induced porphyrin in patients with cervical intraepithelial neoplasia. *Lasers Surg Med.* (2021) 53:654–63. doi: 10.1002/lsm.23338

79. Morisawa S, Jobu K, Ishida T, Kawada K, Fukuda H, Kawanishi Y, et al. Association of 5-aminolevulinic acid with intraoperative hypotension in Malignant glioma surgery. *Photodiagnosis Photodyn Ther.* (2022) 37:102657. doi: 10.1016/j.pdpdt.2021.102657

80. Krupka M, Bartusik-Aebisher D, Strzelczyk N, Latos M, Sieron A, Cieslar G, et al. The role of autofluorescence, photodynamic diagnosis and Photodynamic therapy in Malignant tumors of the duodenum. *Photodiagnosis Photodyn Ther.* (2020) 32:101981. doi: 10.1016/j.pdpdt.2020.101981

81. Buzalewicz I, Holowacz I, Ulatowska-Jarza A, Podbielska H. Towards dosimetry for photodynamic diagnosis with the low-level dose of photosensitizer. *J Photochem Photobiol B.* (2017) 173:333–43. doi: 10.1016/j.jphotobiol.2017.06.007

82. Singh P, Pandit S, Mokkapati V, Garg A, Ravikumar V, Mijakovic I. Gold nanoparticles in diagnostics and therapeutics for human cancer. *Int J Mol Sci.* (2018) 19:1979. doi: 10.3390/ijms19071979

83. Simelane NWN, Kruger CA, Abrahamse H. Targeted nanoparticle photodynamic diagnosis and therapy of colorectal cancer. *Int J Mol Sci.* (2021) 22:9779. doi: 10.3390/ijms22189779

84. Chen C, Tian R, Zeng Y, Chu C, Liu G. Activatable fluorescence probes for "Turn-on" and ratiometric biosensing and bioimaging: from NIR-I to NIR-II. *Bioconjug Chem.* (2020) 31:276–92. doi: 10.1021/acs.bioconjchem.9b00734

85. Miampamba M, Liu J, Harootunian A, Gale AJ, Baird S, Chen SL, et al. Sensitive *in vivo* visualization of breast cancer using ratiometric protease-activatable fluorescent imaging agent, AVB-620. *Theranostics.* (2017) 7:3369–86. doi: 10.7150/thno.20678

86. Szygula M, Wojciechowski B, Adamek M, Pietrusa A, Kawczyk-Krupka A, Cebula W, et al. Fluorescent diagnosis of urinary bladder cancer—a comparison of two diagnostic modalities. *Photodiagnosis Photodyn Ther.* (2004) 1:23–6. doi: 10.1016/S1572-1000(04)00006-7

87. Kuiper T, van den Broek FJC, Naber AH, van Soest EJ, Scholten P, Mallant-Hent RC, et al. Endoscopic trimodal imaging detects colonic neoplasia as well as stand ard video endoscopy. *Gastroenterology*. (2011) 140:1887–94. doi: 10.1053/ j.gastro.2011.03.008

88. Guck J, Schinkinger S, Lincoln B, Wottawah F, Ebert S, Romeyke M, et al. Optical deformability as an inherent cell marker for testing Malignant transformation and metastatic competence. *Biophys J*. (2005) 88:3689–98. doi: 10.1529/ biophysj.104.045476

89. Strzelczyk N, Kwiatek S, Latos W, Sieroń A, Stanek A. Does the Numerical Colour Value (NCV) correlate with preneoplastic and neoplastic colorectal lesions? *Photodiagnosis Photodyn Ther*. (2018) 23:353–61. doi: 10.1016/j.pdpdt.2018.07.012

90. Kara MA, Bergman JJ. Autofluorescence imaging and narrow-band imaging for the detection of early neoplasia in patients with Barrett's esophagus. *Endoscopy*. (2006) 38:627–31. doi: 10.1055/s-2006-925385

91. Lv X, Wang C, Xie Y. Comparison of diagnostic efficacy between AFI, NBI, and AFI combined with NBI for colonic cancers: A meta-analysis. *Saudi J Gastroenterol*. (2017) 23:82–90. doi: 10.4103/1319-3767.203355

92. Park J, Gao L. Advancements in fluorescence lifetime imaging microscopy Instrumentation: Towards high speed and 3D. *Curr Opin Solid State Mater Sci*. (2024) 30:101147. doi: 10.1016/j.cossms.2024.101147

93. Datta R, Heaster TM, Sharick JT, Gillette AA, Skala MC. Fluorescence lifetime imaging microscopy: fundamentals and advances in instrumentation, analysis, and applications. *J BioMed Opt*. (2020) 25:1–43. doi: 10.1117/1.Jbo.25.7.071203

94. Butte PV, Mamelak AN, Nuno M, Bannykh SI, Black KL, Marcu L. Fluorescence lifetime spectroscopy for guided therapy of brain tumors. *Neuroimage*. (2011) 54 Suppl 1:S125–35. doi: 10.1016/j.neuroimage.2010.11.001

95. Cheng H, Xu H, Peng B, Huang X, Hu Y, Zheng C, et al. Illuminating the future of precision cancer surgery with fluorescence imaging and artificial intelligence convergence. *NPJ Precis Oncol*. (2024) 8(1):196. doi: 10.1038/s41698-024-00699-3

96. Niazi MKK, Parwani AV, Gurcan MN. Digital pathology and artificial intelligence. *Lancet Oncol*. (2019) 20:e253–e61. doi: 10.1016/s1470-2045(19)30154-8

97. Ma Z, Wang F, Wang W, Zhong Y, Dai H. Deep learning for *in vivo* near-infrared imaging. *Proc Natl Acad Sci United States America*. (2021) 118(1): e2021446118. doi: 10.1073/pnas.2021446118

98. Kundu S, Das S, Patra A. Fluorescence correlation spectroscopy and fluorescence lifetime imaging microscopy for deciphering the morphological evolution of supramolecular self-assembly. *Chem Commun (Camb)*. (2023) 59:8017–31. doi: 10.1039/d2cc06607f

99. Aswani KK. Emerging LED technologies for fluorescence microscopy. *Microscopy Today*. (2016) 24:22–7. doi: 10.1017/S1551929516000407

100. Xu C, Wang W, Zhang Z, Ma F, Jiang D, Strzep A, et al. Continuous-wave orange laser at 605.98 nm based on a diode-pumped Pr,G d:SrF2 crystal. *Optics Laser Technol*. (2024) 168:109768. doi: 10.1016/j.optlastec.2023.109768

101. Zorin I, Gattinger P, Ebner A, Brandstetter M. Advances in mid-infrared spectroscopy enabled by supercontinuum laser sources. *Optics express*. (2022) 30:5222–54. doi: 10.1364/oe.447269

102. Eisaman MD, Fan J, Migdall A, Polyakov SV. Invited review article: Single-photon sources and detectors. *Rev Sci Instrum*. (2011) 82:071101. doi: 10.1063/ 1.3610677

103. Pietro WJ, Mermut O. A siPM-enabled portable delayed fluorescence photon counting device: climatic plant stress biosensing. *Biosensors*. (2022) 12:817. doi: 10.3390/bios12100817

104. Allmaras JP, Wollman EE, Beyer AD, Briggs RM, Korzh BA, Bumble B, et al. Demonstration of a thermally coupled row-column SNSPD imaging array. *Nano Lett*. (2020) 20:2163–8. doi: 10.1021/acs.nanolett.0c00246

105. Ma PS, Zhang HF, Zhou X. Aligning superconducting transition-edge sensors by reflected wave intensity measurement. *Sensors (Basel)*. (2023) 23:3495. doi: 10.3390/ s23073495

106. Ortega-Ojeda F, Calcerrada M, Ferrero A, Campos J, Garcia-Ruiz C. Measuring the human ultra-weak photon emission distribution using an electron-multiplying, charge-coupled device as a sensor. *Sensors (Basel)*. (2018) 18:1152. doi: 10.3390/ s18041152

107. DS AV, Lin H, Henderson ER, Samkoe KS, Pogue BW. Review of fluorescence guided surgery systems: identification of key performance capabilities beyond indocyanine green imaging. *J BioMed Opt*. (2016) 21:80901. doi: 10.1117/ 1.Jbo.21.8.080901

108. Schupper AJ, Baron RB, Cheung W, Rodriguez J, Kalkanis SN, Chohan MO, et al. 5-Aminolevulinic acid for enhanced surgical visualization of high-grade gliomas: a prospective, multicenter study. *J Neurosurg*. (2022) 136:1525–34. doi: 10.3171/ 2021.5.Jns21310

109. Tjalma JJJ, Koller M, Linssen MD, Hartmans E, de Jongh SJ, Jorritsma-Smit A, et al. Quantitative fluorescence endoscopy: an innovative endoscopy approach to evaluate neoadjuvant treatment response in locally advanced rectal cancer. *Gut*. (2020) 69:406–10. doi: 10.1136/gutjnl-2019-319755

110. Liu L, Nie Y, Lin L, Li W, Huang Z, Xie S, et al. Pattern recognition of multiple excitation autofluorescence spectra for colon tissue classification. *Photodiagnosis Photodyn Ther*. (2013) 10:111–9. doi: 10.1016/j.pdpdt.2012.07.003

111. Schuty B, Martínez S, Guerra A, Lecumberry F, Magliano J, Malacrida L. Quantitative melanoma diagnosis using spectral phasor analysis of hyperspectral imaging from label-free slices. *Front Oncol*. (2023) 13:1296826. doi: 10.3389/ fonc.2023.1296826

112. Adir O, Poley M, Chen G, Froim S, Krinsky N, Shklover J, et al. Integrating artificial intelligence and nanotechnology for precision cancer medicine. *Advanced materials (Deerfield Beach Fla)*. (2020) 32:e1901989. doi: 10.1002/adma.201901989

113. Hardy NP, Epperlein JP, Dalli J, Robertson W, Liddy R, Aird JJ, et al. Real-time administration of indocyanine green in combination with computer vision and artificial intelligence for the identification and delineation of colorectal liver metastases. *Surg Open science*. (2023) 12:48–54. doi: 10.1016/j.sopen.2023.03.004

114. Heidari AE, Pham TT, Ifegwu I, Burwell R, Armstrong WB, Tjoson T, et al. The use of optical coherence tomography and convolutional neural networks to distinguish normal and abnormal oral mucosa. *J biophotonics*. (2020) 13:e201900221. doi: 10.1002/ jbio.201900221